Heliyon

ELSEVIER

Received:
30 May 2018
Revised:
16 September 2018
Accepted:
5 December 2018

Cite as: Abdullah Shah, Sadia Saeed, Saher Akmal Khan. Numerical investigation of bubbles coalescence in a shear flow with diffuse-interface model. Heliyon 4 (2018) e01024. doi: 10.1016/j.heliyon.2018.e01024

Numerical investigation of bubbles coalescence in a shear flow with diffuse-interface model

Abdullah Shah [a,b,*], **Sadia Saeed** [a], **Saher Akmal Khan** [a]

[a] *Department of Mathematics, COMSATS University Islamabad, Park Road, Islamabad-45550, Pakistan*

[b] *LSEC and Institute of Computational Mathematics and Scientific/Engineering Computing, Academy of Mathematics & Systems Science, Chinese Academy of Sciences, Beijing 100190, PR China*

* Corresponding author at: Department of Mathematics, COMSATS University Islamabad, Park Road, Islamabad-45550, Pakistan.
E-mail address: abdullah_shah@comsats.edu.pk (A. Shah).

Abstract

In this article, we apply the diffuse-interface model [developed by Shah and Yuan (2011) [21]] for collision and coalescence of two bubbles in a linear shear flow. The governing equations consist of a system of coupled nonlinear partial differential equations for conservation of mass, momentum and phase transport. In the two-phase flow, the diffuse-interface model relaxes certain numerical difficulties for tracking the moving interface. An artificial compressibility based numerical scheme is implemented to study the effects of surface tension on bubbles coalescence and separation. We found the critical value of the surface tension coefficient and observed that lowering the surface tension coefficient from the critical value prevent bubbles to coalesce.

Keywords: Computational mathematics

1. Introduction

In recent years, prediction and understanding of the conditions for coalescence and non-coalescence of bubbles in a shear flow are found to be very important in many

https://doi.org/10.1016/j.heliyon.2018.e01024

industrial processes like lab-on-a-chip [1], oil recovery [2], ink-jet printing [3] and surfactant emulsion [4] etc. The presence of surfactant substances may greatly affect the physical properties of the fluid mixture. In fact, these effects are crucial in many real-world applications. Surfactant molecules are used to reduce surface tension by interacting with the bonding forces between fluid molecules. For example, detergents make water wetter, and emulsifiers stabilize emulsions by preventing small bubbles to coalesce [5]. Since as in coalescence, the fluid between two bubbles drains as they approach each other and if this drainage proceeds sufficiently long, the film between the bubbles turns out to be adequately thin, a bridge is formed because inter-molecular forces become dominant. This bridge grows due to surface tension and bubbles coalescence.

Two-phase flow in shear driven channels has gained much attention because of its wide applicability in modern science and technology applications. In two-phase flow, each phase has its own physical properties (density, viscosity and concentration etc.) which are uniform within the occupied domain. As fluids are mixed, physical properties may change in a discontinuous way across the interface. The interfacial tension dominates the behavior of the two-phase flows phenomena at a very small scale. Numerical simulations are used to understand the complex phenomenon of two-phase flow. There are many different numerical methods to incorporate the surface tension in two-phase flows. For example, front-tracking methods [6, 7] uses the Lagrangian particles to track the interfaces. Since merging and breaking of bubbles involves interface breakup, the front tracking methods require excessive processing time. There, these methods are not that suitable for the simulation of such type of problems. On the other hand, front-capturing method capture the interface on regular fixed stationary grids. The most popular examples of front-capturing methods are the volume-of-fluid (VOF) [8, 9], the level-set (LS) [10, 11, 12, 13, 14] and the phase-field methods [15, 16, 17, 18, 19, 20, 21, 22]. The diffuse interface model replaces the singularity at the interface by a smooth function with some transition region. In this thin transition region, the two components are mixed and store a certain amount of energy. The free energy is defined by the phase function ϕ, which track the evolution of the interface by solving a time-dependent convection–diffusion equation. Due to the enormous simplicity in modeling and ease in coding, the diffuse interface model (also known as the phase-field model) has become an increasingly popular choice for solving multi-phase flow problems. The advantages of the phase-field models over others are; (i) relatively easy to construct using simple symmetry arguments and conservation laws; (ii) systematic development of the continuum limit which makes mesoscopic and macroscopic time and length scales accessible; (iii) natural emergence of interfaces and non-equilibrium conditions; (iv) relative ease of numerical implementation and; (v) possibility for analytical work through projection techniques [23].

 https://doi.org/10.1016/j.heliyon.2018.e01024

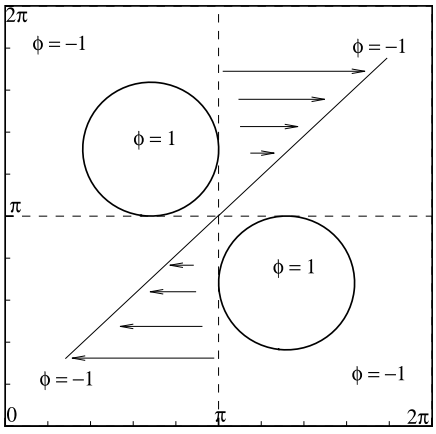

Figure 1. Geometry of the two bubbles in a linear shear flow.

In incompressible two-phase flows, the physical variables required to describe the motion are velocity, pressure, density, viscosity, surface tension, and buoyancy force. The surface tension is an important quantity of fluids and its variation has interesting effects on the flow-field. Generally, to obtain the velocity and pressure of the fluid, Navier–Stokes equations are solved numerically by using different discretization schemes such as the finite difference, the finite element or the finite volume schemes. The dynamics of phase transport is governed either by Allen–Cahn equation [24] or Cahn–Hilliard equation [25]. The difference between both is that the $2nd$-order Allen–Cahn equation is not mass conserving while the $4th$-order Cahn–Hilliard equation naturally satisfy the mass conservation. We used the modified Allen–Cahn equation which is not only the mass preserving but also gives the ease in coupling with artificial compressibility formulation of Navier–Stokes equations. Based on the phase-field model proposed by Liu and Shen [26], Shah and Yuan [21] has proposed a numerical method for the two-phase incompressible coupled system which is based on the artificial compressibility method in two- and three-dimensions. In this paper, we study the collision, coalescing and non-coalescing of two bubbles in a linear shear flow. The coalescence processes usually occur in three stages. Initially, the bubbles collide then the drainage of the liquid film occurs and finally film rapture, leading to a bigger bubble. Similar studies that use the phase-field model to capture the interface dynamics have been conducted. Badalassi et al. [27] solved the problem of one bubble in a shear flow by using high-resolution schemes for the convective Cahn–Hilliard equation whereas Yue et al. [28] tested their semi-implicit Fourier spectral method for one drop deformation in a shear flows. A schematic diagram of the coalescence problem is shown in Figure 1. Two initially circular bubbles of radius 1.0 are initialized with a shear flow rate [29] $u = \frac{1}{\pi}(y - \pi)$. The effects of density or viscosity differences between the two phases are studied. Therefore both phases have the same density ρ and viscosity ν constants.

 https://doi.org/10.1016/j.heliyon.2018.e01024

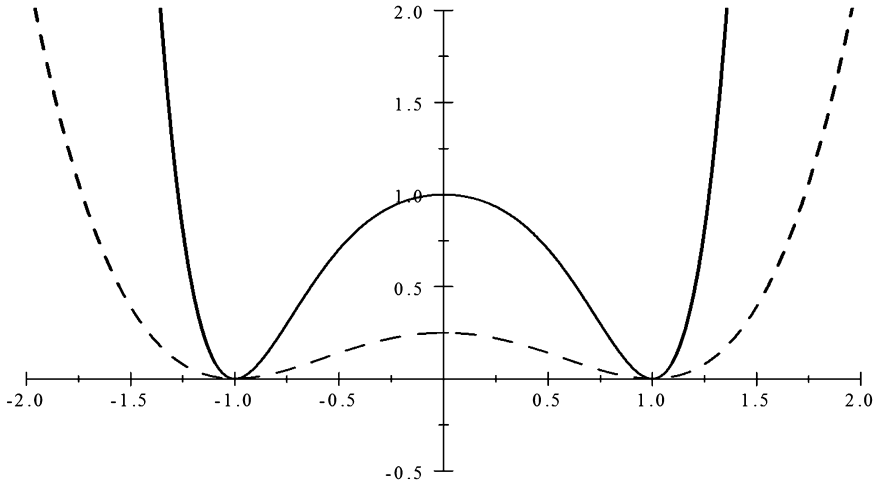

Figure 2. The double-well potentials for $\eta = 1$ (a) $F(\phi) = \frac{1}{4}(\phi^2 - 1)^2$ (dash line) and $F(\phi) = \phi^6 - \phi^4 - \phi^2 + 1$ (solid line).

This paper is organized as follows. The governing equation and solution methods are given in Section 2. In Section 3, numerical simulations are performed and results are illustrated graphically. Section 4 concludes this paper.

2. Methodology

2.1. Phase-field equations

Let Ω be the domain occupied by the system, then the total free energy is defined as;

$$E(\phi, \nabla\phi) = \int_{\Omega} (\frac{1}{2} \mid \nabla\phi \mid^2 + F(\phi)) d\Omega. \tag{1}$$

The gradient energy term is zero inside the phases but is nonzero across the interface. In Eq. (1), $F(\phi)$ is the double-well potential which has with two real minima at $\phi = \pm 1$ i.e.,

$$F(\phi) = \frac{1}{4\eta^2}(\phi^2 - 1)^2, \tag{2}$$

where η is the interfacial width. Another option for the double-well potential [30] is

$$F(\phi) = \phi^6 - \phi^4 - \phi^2 + 1. \tag{3}$$

However due to the higher-order polynomial in Eq. (3), the nonlinearity ($F'(\phi)$) will increase making more time step restrictions. Therefore, we have used the comparatively more simple potential $F(\phi)$ given in Eq. (2) and is shown in Figure 2.

The functional derivative of free energy with respect to order parameter is the chemical potential μ of the mixture, defined as,

$$\mu = \frac{\delta E}{\delta \phi} = F'(\phi) - \Delta\phi.$$

A minimum in E is given by:

$$\frac{\delta E}{\delta \phi} = 0 \Rightarrow F'(\phi) - \Delta\phi = 0,$$

which is a $2nd$-order nonlinear differential equation with a solution of the form

$$\phi(\mathbf{x}) = \tanh\left(\frac{\mathbf{x}}{\sqrt{2}\eta}\right),$$

satisfying the boundary condition $\phi(\pm 1) = \pm 1$. The momentum equation can be described:

$$\rho_0\left[\mathbf{u}_t + (\mathbf{u}\cdot\nabla)\mathbf{u}\right] = -\nabla\tilde{p} + \nabla\cdot\sigma,$$

Stress tensor (viscous + elastic) σ is given by

$$\sigma = \mu(\phi)\left[\nabla\mathbf{u} + (\nabla\mathbf{u})^T\right] - \lambda\nabla\phi\otimes\nabla\phi,$$

and the viscosity coefficient is, $\mu(\phi) = \frac{1+\phi}{2}\mu_1 + \frac{1-\phi}{2}\mu_2$ and surface tension coefficient is λ.

2.2. Conservative Allen–Cahn equation

In phase-field method, determination of phase-field variables or order parameters is the most important step. Usually order parameters are categorized into conserved and non-conserved. Although there is no systematic way to choose these order parameters, but it is usually enough for them to describe the morphology and total free energy of complex microstructure, qualitatively. In order to simulate the spatial and temporal evolution, the non-conserved parameters governed by the Allen–Cahn equation is defined as

$$\phi_t + (\mathbf{u}.\nabla)\phi = -\gamma\frac{\delta E}{\delta\phi} = \gamma(\Delta\phi - f(\phi)) \tag{4}$$

Here, γ is the elastic relaxation time or the mobility of order parameter and $f(\phi) = F'(\phi)$. Rubinstein and Sternberg [31] introduced a time dependent Lagrange multiplier $\xi(t)$ to ensure the conservation of mass of Eq. (4) as

$$\phi_t + (\mathbf{u}.\nabla)\phi = \gamma(\Delta\phi - f(\phi) + \xi(t)).$$

We used the formula for $\xi(t)$ derived by Di et al. [24] to keep the maximal principle for ϕ.

2.3. Governing equations

The governing equation consists of unsteady, incompressible ($\rho = 1$ for simplicity and same viscosity), coupled and nonlinear set of the following equations:

$$\nabla.\mathbf{u} = 0, \tag{5}$$

$$\mathbf{u}_t + (\mathbf{u}.\nabla)\mathbf{u} + \nabla p - \nabla.[\mu(\nabla\mathbf{u} + (\nabla\mathbf{u})^T)] = -\lambda\Delta\phi\nabla\phi, \tag{6}$$

$$\phi_t + (\mathbf{u}.\nabla)\phi - \gamma\Delta\phi = \gamma(\xi(t) - f(\phi)). \tag{7}$$

The following initial conditions

$$\mathbf{u}|_{t=0} = \mathbf{u}_0, \quad \phi|_{t=0} = \phi_0, \tag{8}$$

and appropriate boundary conditions

$$\mathbf{u}|_{\partial\Omega} = 0, \quad \frac{\partial\phi}{\partial n}\,|_{\partial\Omega} = 0 \tag{9}$$

are used. Here, $\mathbf{u} = (u, v)$ is velocity vector, and p represent the pressure.

2.4. Artificial compressibility method

Incompressible flows are governed by continuity and momentum equations. These equations are difficult to solve analytically due to nonlinear convective terms in momentum equations and absence of pressure term in the continuity equation. Chorin [32] has proposed artificial compressibility method by adding time derivative of pressure to the continuity equation. By combining Eq. (5), Eq. (6) and Eq. (7) with artificial compressibility method as follows;

$$\frac{\partial p}{\partial\tau} + \beta(\frac{\partial u}{\partial x} + \frac{\partial v}{\partial y}) = 0, \tag{10}$$

$$\frac{\partial u}{\partial\tau} + \frac{\partial u}{\partial t} + \frac{\partial(u^2+p)}{\partial x} + \frac{\partial uv}{\partial y} - \mu(\frac{\partial^2 u}{\partial x^2} + \frac{\partial^2 u}{\partial y^2}) = -\lambda\frac{\partial\phi}{\partial x}(\frac{\partial^2\phi}{\partial x^2} + \frac{\partial^2\phi}{\partial y^2}), \tag{11}$$

$$\frac{\partial v}{\partial\tau} + \frac{\partial v}{\partial t} + \frac{\partial uv}{\partial x} + \frac{\partial(v^2+p)}{\partial y} - \mu(\frac{\partial^2 v}{\partial x^2} + \frac{\partial^2 v}{\partial y^2}) = -\lambda\frac{\partial\phi}{\partial y}(\frac{\partial^2\phi}{\partial x^2} + \frac{\partial^2\phi}{\partial y^2}), \tag{12}$$

$$\frac{\partial\phi}{\partial\tau} + \frac{\partial\phi}{\partial t} + \frac{\partial(u\phi)}{\partial x} + \frac{\partial(v\phi)}{\partial y} - \gamma(\frac{\partial^2\phi}{\partial x^2} + \frac{\partial^2\phi}{\partial y^2}) = \gamma(1-\phi^2)(\frac{\phi}{\eta^2} + \xi(t)). \tag{13}$$

The artificial compressibility factor β is chosen in such a way that incompressibility condition is satisfied when steady state is reached. Writing the above Eqs. (10)–(13) in conservative form as

$$Q_\tau + I_m Q_t + (E - E_v)_x + (F - F_v)_y = S_{int}, \tag{14}$$

with initial and boundary conditions given in Eq. (8) and Eq. (9). In Eq. (14), Q is the solution vector, γ is the elastic relaxation time, β is the artificial compressibility factor, τ is the pseudo-time and t is the physical time. The I_m is the modified identity

matrix comes when we write conservative form of our governing Eqs. (10)–(13). The S_{int} is the source term on the right hand side of the governing equations. The discretization techniques and solution algorithm developed by Shah and Yuan [21] is used for the purpose of numerical simulation in the next section. The main advantage of this formulation and method is that (i) the formulation is in primitive variables (ii) it is implicit so time step restriction is relaxed (iii) and its extension to 3D is very straight-forward.

3. Results & Discussions

In this section, the numerical simulations are performed for different values of surface tension coefficient λ while keeping other parameters fixed i.e., $\mu = \gamma = 0.023$, $\eta = 0.02$ and computational domain is a square of $[0, 2\pi] \times [0, 2\pi]$ which discretized with uniform mesh of size 321×321. For the sake of simplicity, we present results only for $\lambda = 0.02$ (coalescence) and $\lambda = 0.01$ (non-coalescence). The physical time step is $\Delta t = 0.005$, pseudo-time step $\Delta\tau$ is determined based on a CFL number of 5, the maximum number of sub-iteration = 100 and $\beta = 200$. The initial velocity field $(u, v) = (\frac{1}{\pi}(y - \pi), 0)$, pressure is extrapolated from the interior, while the initial condition for phase function ϕ is specified as follows;

$$\phi(\mathbf{x}, 0) = \begin{cases} \tanh\left(\dfrac{1 - \|\mathbf{x} - \mathbf{x}_1\|}{\sqrt{2}\eta}\right) & \|\mathbf{x} - \mathbf{x}_1\| < 1 + \sqrt{2}\eta \\ \tanh\left(\dfrac{1 - \|\mathbf{x} - \mathbf{x}_2\|}{\sqrt{2}\eta}\right) & \|\mathbf{x} - \mathbf{x}_2\| < 1 + \sqrt{2}\eta \\ -1 & \text{otherwise} \end{cases}$$

so that $\phi = 1$ inside the two bubbles of radii 1 having center at $\mathbf{x}_1 = (2.14, 4.14)$ and $\mathbf{x}_2 = (4.14, 2.14)$ and $\phi = -1$ in the surrounding fluid.

3.1. Bubbles coalescence

In a shear driven flow, the two bubbles initially come closer, collide and then coalescence occurs for surface tension coefficient greater than a critical value [29]. In our first experiment for $\lambda = 0.02$, as the simulation begin, the two bubbles start moving towards each other with a given velocity till the collision occurs at $t \simeq 2.75$ as shown in Figures 3(a–d), then they start merging to form a larger bubble, the fluid between them drains having the deformation shown in Figures 3(e–h). The coalescence between the bubbles depends upon the value of the surface tension coefficient. Also as the system evolved, the effect of the Lagrange multiplier used in the Allen–Cahn equation can be seen clearly so that the newly formed bubble has the mass conserving property [21].

https://doi.org/10.1016/j.heliyon.2018.e01024

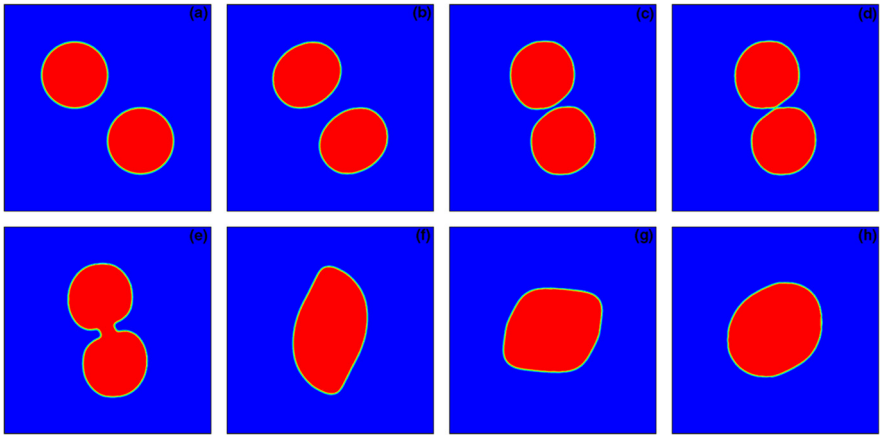

Figure 3. Evolution of two interacting bubbles in a linear shear flow from (a–h) at time $t = 0.0, 1.0, 2.5, 2.75, 2.85, 4.0, 5.0\ 10.0$ respectively for $\lambda = 0.02$. It can be seen that the two bubbles come closer and merge at $t = 2.75$ approximately.

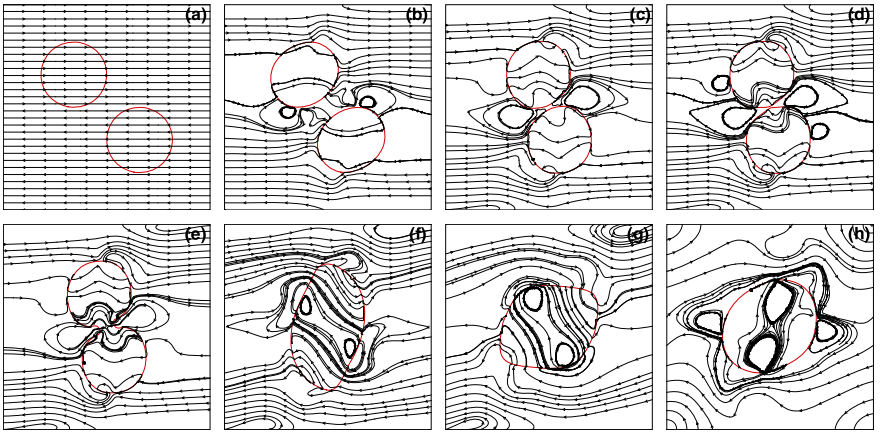

Figure 4. Complex flow (streamline contours) for the two bubbles from (a–h) at time $t = 0.0, 1.0, 2.5, 2.75, 2.85, 4.0, 5.0\ 10.0$ respectively for $\lambda = 0.02$.

In Figures 4(a–h), the streamline contours are given to show the effect of surface tension in a shear flow. Initially, the flow-field is linear in Figure 4(a), as the time passes, the flow-field becomes more turbulent in the vicinity of the interaction of the two bubbles and becomes stronger and much more complex as shown in Figures 4(b–h). The appearance and growth of different convection cells is due to the motion of two bubbles towards each other.

3.2. Non-coalescence of bubbles

The next simulation is for $\lambda = 0.01$, where initially the two bubbles came closer to each other with a given velocity. However, they do not drain but slide over each other

 https://doi.org/10.1016/j.heliyon.2018.e01024

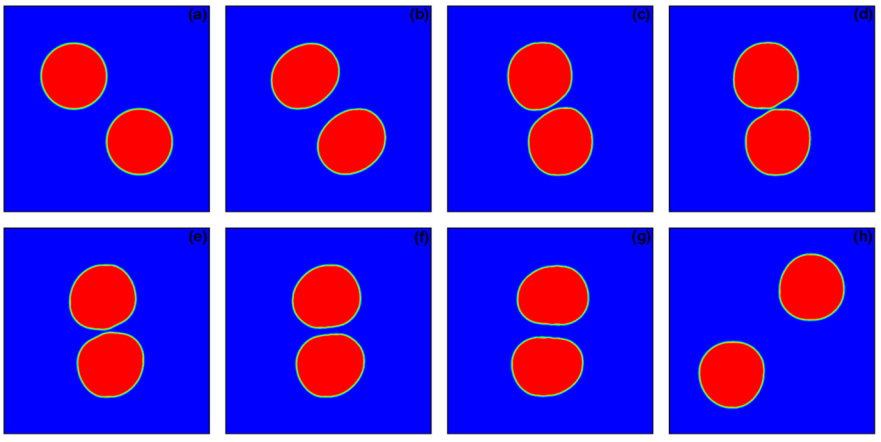

Figure 5. Evolution of two interacting bubbles in a linear shear flow from (a–h) at time $t = 0.0, 1.0, 2.50, 3.0, 3.25, 3.5, 4.0, 7.5$ respectively for $\lambda = 0.01$, having no coalescence.

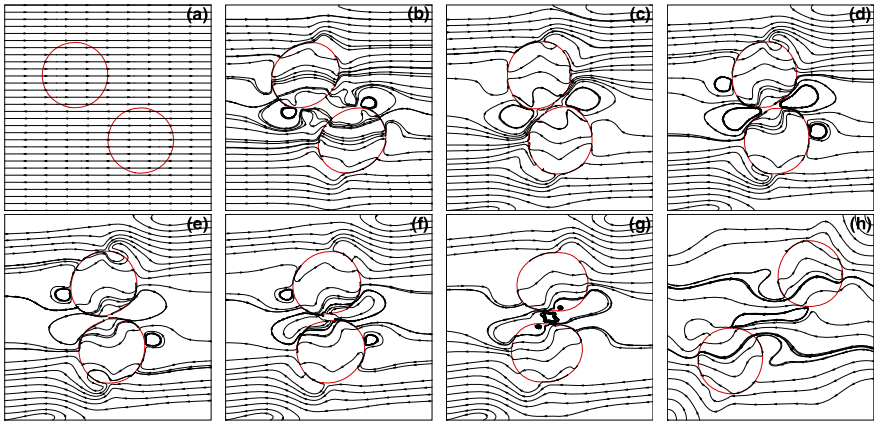

Figure 6. Complex flow (streamline contours) for two bubbles from (a–h) at time $t = 0.0, 1.0, 2.50, 3.0, 3.25, 3.5, 4.0, 7.5$ respectively for $\lambda = 0.01$.

as shown in Figures 5(a–h). It is observed that there is a critical value $\lambda_c \epsilon (0.02, 0.01)$ such that for $\lambda < \lambda_c$, there is no coalescence while $\lambda > \lambda_c$, the coalescence occurs.

In Figures 6(a–h), the streamline contours are given to show the effect of surface tension in a shear flow. Initially from a linear flow-field Figure 6(a) to a more turbulent flow-field in the vicinity of the interaction of the two bubbles as shown in Figures 6(b–h).

4. Conclusion

We have discussed the application of a the phase-field method to model two-phase flows by solving a coupled system of incompressible Navier–Stoke equations and phase-field equation numerically. We have shown the effect of surface tension in a simple linear shear flow. From the simulation results, it is observed that for $\lambda = 0.02$,

https://doi.org/10.1016/j.heliyon.2018.e01024

the coalescence of bubbles occur and then by lowering i.e., for $\lambda = 0.01$, the bubbles show a non-coalesce behavior. Therefore, it is concluded that the critical values for coalescence and non-coalescence is between $\lambda = 0.02$ and $\lambda = 0.01$. In our future work, we want to add the effect of surfactant [29] in our present model to study the interfacial tension of the two-phase flow.

Declarations

Author contribution statement

Abdullah Shah: Conceived and designed the experiments; Wrote the paper.

Sadia Saeed: Conceived and designed the experiments; Performed the experiments; Analyzed and interpreted the data; Contributed reagents, materials, analysis tools or data; Wrote the paper.

Saher A. Khan: Performed the experiments; Analyzed and interpreted the data; Contributed reagents, materials, analysis tools or data.

Funding statement

This research did not receive any specific grant from funding agencies in the public, commercial, or not-for-profit sectors.

Competing interest statement

The authors declare no conflict of interest.

Additional information

No additional information is available for this paper.

Acknowledgements

Part of this work was carried out while A. Shah was visiting ICMSEC, Chinese Academy of Sciences, Beijing China as a PIFI visiting scientist. Suggestions and support of Prof. Li Yuan is highly acknowledged.

References

[1] H.A. Stone, A.D. Stroock, A. Ajdari, Engineering flows in small devices: microfluidics toward a lab-on-a-chip, Annu. Rev. Fluid Mech. 36 (2004) 381–411.

[2] J.S. Eow, M. Ghadiri, Electrostatic enhancement of coalescence of water droplets in oil: a review of the technology, Chem. Eng. J. 85 (2002) 357–368.

[3] B. Zhang, J. He, X. Li, F. Xu, D. Li, Micro/nanoscale electrohydrodynamic printing: from 2D to 3D, Nanoscale 8 (2016) 15376–15388.

[4] D.T. Chiu, A.J. deMello, D. Di Carlo, P.S. Doyle, C. Hansen, R.M. Maceiczyk, R.C.R. Wootton, Small but perfectly formed? Successes, challenges, and opportunities for microfluidics in the chemical and biological sciences, Chem 2 (2017) 201–223.

[5] D.A. Edwards, H. Brenner, D.T. Wasan, Interfacial Transport Processes and Rheology, Butterworth-Heinemann, Boston, 1991.

[6] G. Tryggvason, B. Bunner, A front-tracking method for the computations of multiphase flow, J. Comput. Phys. 169 (2001) 708–759.

[7] S.O. Unverdi, G. Tryggvason, A front-tracking method for viscous, incompressible, multi-fluid flows, J. Comput. Phys. 100 (1992) 25–37.

[8] G. Tryggvason Scardovelli, S. Zaleski, Direct Numerical Simulations of Gas-Liquid Multiphase Flows, Cambridge University Press, Cambridge, 2011, Chapter 10.

[9] S. Zaleski, Li Succi, Two-dimensional Navier–Stokes simulation of deformation and breakup of liquid patches, Phys. Rev. Lett. 72 (1995) 244–247.

[10] Shu Osher, Efficient implementation of essentially non-oscillatory shock capturing schemes, J. Comput. Phys. 77 (1988) 439–471.

[11] J.A. Sethian, Level-set methods and fast marching methods, in: Evolving Interfaces in Computational Geometry, Fluid Mechanics, Computer Vision and Materials Science, Cambridge University Press, New York, 1999.

[12] F.J. Smith Solis, L. Tao, K. Thornton, M.O. De La Cruz, Domain growth in ternary fluids: a level set approach, Phys. Rev. Lett. 84 (2000) 91–94.

[13] M. Sussman, A second order coupled level set and volume-of-fluid method for computing growth and collapse of vapor bubbles, J. Comput. Phys. 187 (2003) 110–136.

[14] M. Pathak, Numerical analysis of droplet dynamics under different temperature and cross-flow velocity conditions, ASME J. Fluids Eng. 134 (2012) 0445011-0445016.

[15] D.M. Anderson, G.B. McFadden, A.A. Wheeler, Diffuse-interface methods in fluid mechanics, Annu. Rev. Fluid Mech. 30 (1998) 139–165.

[16] H.-G. Lee, J.S. Lowengrub, J. Goodman, Modeling pinchoff and reconnection in a Hele-Shaw cell. I. The models and their calibration, Phys. Fluids 14 (2002) 492–513.

[17] J. Kim, K. Kang, J. Lowengrub, Conservative multigrid methods for Cahn–Hilliard fluids, J. Comput. Phys. 193 (2004) 511–543.

[18] J. Kim, A diffuse-interface model for axisymmetric immiscible two-phase flow, Appl. Math. Comput. 160 (2005) 589–606.

[19] H. Ding, P.D.M. Spelt, Wetting condition in diffuse interface simulations of contact line motion, Phys. Rev. E 75 (2007) 2078–2095.

[20] J. Shen, X. Yang, An efficient moving mesh spectral method for the phase-field model of two-phase flows, J. Comput. Phys. 228 (2009) 2978–2992.

[21] A. Shah, L. Yuan, Numerical solution of a phase-field model for incompressible two-phase flows based on artificial compressibility, Comput. Fluids 42 (2011) 54–61.

[22] A. Shah, S. Saeed, L. Yuan, An artificial compressibility method for 3D phase-field model and its application to two-phase flows, Int. J. Comput. Methods 14 (2) (2017) 1750059-14.

[23] V. Heinonen, C.V. Achim, K.R. Elder, T. Ala-Nissila, Phase-field-crystal models and mechanical equilibrium, Phys. Rev. E 89 (2014) 032411-11.

[24] Y.N. Di, R. Li, T. Tang, General moving mesh framework in 3D and its application for simulating the mixture of multi-phase flows, Commun. Comput. Phys. 3 (2008) 582–602.

[25] J.W. Cahn, J.E. Hilliard, Free energy of a nonuniform system. I. Interfacial free energy, J. Chem. Phys. 28 (1958) 258–267.

[26] C. Liu, j. Shen, A phase field model for the mixture of two incompressible fluids and its approximation by a Fourier-spectral method, Phys. D: Nonlinear Phenom. 179 (3–4) (2003) 211–228.

[27] V.E. Badalassi, H.D. Ceniceros, Sanjoy Banerjee, Computation of multiphase systems with phase field models, J. Comput. Phys. 190 (2) (2003) 371–397.

[28] P. Yue, J.J. Feng, C. Liu, J. Shen, A diffuse-interface method for simulating twophase flows of complex fluids, J. Fluid Mech. 515 (2004) 293–317.

[29] S. Engblom, M. Do-Quang, G. Amberg, A. Tornberg, On diffuse interface modeling and simulation of surfactants in two-phase fluid flow, Commun. Comput. Phys. 14 (4) (2013) 879–915.

[30] A. Shah, M. Sabir, M. Qasim, P. Bastain, Efficient numerical scheme for solving the Allen–Cahn equation, Numer. Methods Partial Differ. Equ. 34 (5) (2018) 1820–1833.

[31] J. Rubinstein, P. Sternberg, Nonlocal reaction–diffusion equations and nucleation, IMA J. Appl. Math. 48 (1992) 249–264.

[32] A.J. Chorin, A numerical method for solving incompressible viscous flow problems, J. Comput. Phys. 2 (1967) 12–26.